N71-27662

NASA TECHNICAL MEMORANDUM

NASA TM X-62,031

NASA TM X-62,031

CASE FILE COPY

ESTIMATION OF SHOCK LAYER THICKNESS AND PRESSURE DISTRIBUTION ON A DELTA WING–BODY SPACE SHUTTLE ORBITER

George E. Kaattari

Ames Research Center
Moffett Field, Calif. 94035

May 1971

ERRATA

NASA TM X-62,031

By George E. Kaattari

Figure 1.- $\tan\varepsilon_y$ should be $\tan\varepsilon_z$ and $\cos\varepsilon_z$ should be $\cos\varepsilon_y$

Figure 4.- ε_y should be ε_z

Issued 5-19-71

ESTIMATION OF SHOCK LAYER THICKNESS AND PRESSURE DISTRIBUTION ON A DELTA WING-BODY SPACE SHUTTLE ORBITER

By

George E. Kaattari
Ames Research Center

SUMMARY

Methods are presented for calculation of both the shock inclination angle and the surface pressure coefficient in the vertical plane of symmetry of bodies at angle of attack. The methods are applicable over an angle of attack range from 0° to a maximum angle that depends on the body slenderness ratio; for very slender bodies, this maximum angle of attack approaches 90°. The methods apply to configurations of elliptical cross section and of rectangular cross section with rounded corners.

INTRODUCTION

There is much interest currently in pressures and shock layer thicknesses generated on bodies at large angles of attack during atmosphere entry. Theoretical solutions, refs. 1 and 2, have been developed for pressure distributions and shock layer thicknesses for symmetrical profiles at zero angle of attack. More recent works, typically refs. 3 and 4, have considered the nonsymmetric flow cases of bodies at angle of attack. These are all numerical solutions of exact equations and, except in ref. 3, require that the body be a simple analytic shape. Approximate pressure distributions have been computed for more general (nonanalytic) shapes such as wing-body combinations by tangent wedge and tangent circular cone methods and by Newtonian theory.

The present method for estimating the shock locations and surface pressure coefficients in the vertical plane of symmetry is developed by analysis of a simple cone at angle of attack. The method may be extended, however, to the prediction of symmetry plane pressures and shock layer thicknesses of configurations with arbitrarily varying (and expanding) cross sections. This extension to the method is accomplished by approximation of the body with a tandem series of cone frustums of appropriate cross section. In effect, this then is a tangent cone method but differs from the standard technique in that the tangent cone can be made to closely coincide with the entire windward local body periphery in the spanwise direction. This requirement is not possible with a circular cone which can be tangent only to a point on the body and thus cannot give a realistic shock layer thickness. The present method, moreover, is applicable to a larger angle-of-attack range than is the method of the tangent circular cone.

a	semiminor axis of an ellipse
b	semimajor axis of an ellipse or semispan of a slab section
C_p	surface pressure coefficient
C_{p_θ}	pressure coefficient behind oblique shock inclined θ degrees with respect to free-stream direction
k	parameter defined by equation (3)
l	length of cone
M_o	free-stream Mach number
m	virtual shock element (sketch (a))
n	element of actual shock
P	surface pressure on cone plane of symmetry
P_o	free-stream pressure
P_θ	pressure behind oblique shock inclined θ degrees to free-stream direction
q_o	free-stream dynamic pressure
r_c	corner radius of slab section
s	length along body surface from nose apex (figure 3)
V_o	free-stream velocity
$\overline{V}_y$	average velocity normal to shock in shock layer
X	axis tangent to oblique shock (sketch (a))
x_o	cone base reference length in X-direction
Y	axis normal to oblique shock (sketch (a))

α	angle of attack
β	angle between shock and cone surface
γ	specific heat ratio of gas
Δ_o	shock standoff distance for yawed cylinders
Δ_s	shock standoff distance on arbitrary body at location s
ΔP	pressure increment between shock and yawed cylinder surface in plane of symmetry
Δx	length increment of transformed body (sketch (a))
ε_y	semiapex angle of cone in minor axis plane
ε_z	semiapex angle of cone in major axis plane
θ	inclination angle of shock to free-stream direction
ρ_o	free-stream gas density
ρ_θ	gas density behind oblique shock inclined θ degrees to free-stream direction

ANALYSIS

The analysis will be developed in two parts. The first part will discuss a semi-empirical equation used to calculate the pressure coefficient in the vertical plane of symmetry on a conical body of arbitrary cross section at angle of attack. The equation is a function of the free-stream flow properties, the shock inclination angle, θ, and the differential angle, β, between the shock trace and the body surface in the vertical plane of symmetry. The second part presents a means of calculating the angle, β, as a function of angle of attack, α, for conical bodies having two types of body cross-section.

Pressure Coefficient

The pressure coefficient for a perfect gas behind an oblique shock at angle θ is

$$\frac{P_\theta - P_o}{q_o} = C_{p_\theta} = \frac{4}{(\gamma+1)}\left(\sin^2\theta - \frac{1}{M_o^2}\right) \quad \ldots\ldots\ldots\ldots (1)$$

When the oblique shock is associated with a wedge (two-dimensional flow), the angle between the wedge and shock is $\beta = \tan^{-1}\left(\frac{\rho_o}{\rho_\theta}\tan\theta\right)$, where $\frac{\rho_o}{\rho_\theta}$ is the reciprocal shock density ratio across the oblique shock. The pressure coefficient on the wedge is identical to C_{p_θ} (equation (1)).

If the shock is associated with an infinitely long ($\varepsilon_y = 0$) yawed cylinder, the shock trace is parallel to the cylinder and $\beta = 0$. The pressure coefficient on the cylinder is then due to the stagnation pressure corresponding to the normal Mach number, $M_o\sin\theta$. The increase in pressure coefficient from the shock to the cylinder surface may be determined with the aid of shock tables. For normal Mach numbers, greater than 2.5, this pressure coefficient increase is given to a good approximation (within 6%) by-

$$\frac{\Delta P}{q_o} = \frac{\rho_o}{\rho_\theta}\sin^2\theta = \frac{\gamma-1}{\gamma+1}\sin^2\theta + \frac{2}{(\gamma+1)M_o^2} \quad \ldots\ldots\ldots\ldots (2)$$

It is assumed that the variation in the surface pressure coefficient between the limiting cases of a wedge and a yawed cylinder is a linear function of the parameter, k, defined below

$$k = \frac{\tan\beta}{\frac{\rho_o}{\rho_\theta}\tan\theta} \quad \ldots\ldots\ldots\ldots\ldots\ldots (3)$$

The "generalized" pressure coefficient is then

$$C_p = C_{p_{\theta}} + \frac{\Delta P}{q_{o_{\theta}}} (1-k) \quad \ldots\ldots\ldots\ldots\ldots\ldots \quad (4)$$

Equations (1), (2), and (3) when combined with equation (4) results in-

$$C_p = \frac{(\gamma+3)}{(\gamma+1)} \sin^2\theta - \frac{2}{(\gamma+1)M_o^2} - \sin\theta\cos\theta\tan\beta \quad \ldots\ldots\ldots\ldots\ldots\ldots (5)$$

Shock and Body Angle Relationships

Equation (5) developed in the preceding section presumes a known relationship between the angles, θ and β. This relationship is not generally available from existing theories for conical bodies of arbitrary cross section at angle of attack. This section, therefore, describes a method by which the shock and body angle relationships may be determined by simple calculations involving two-dimensional shock theory.

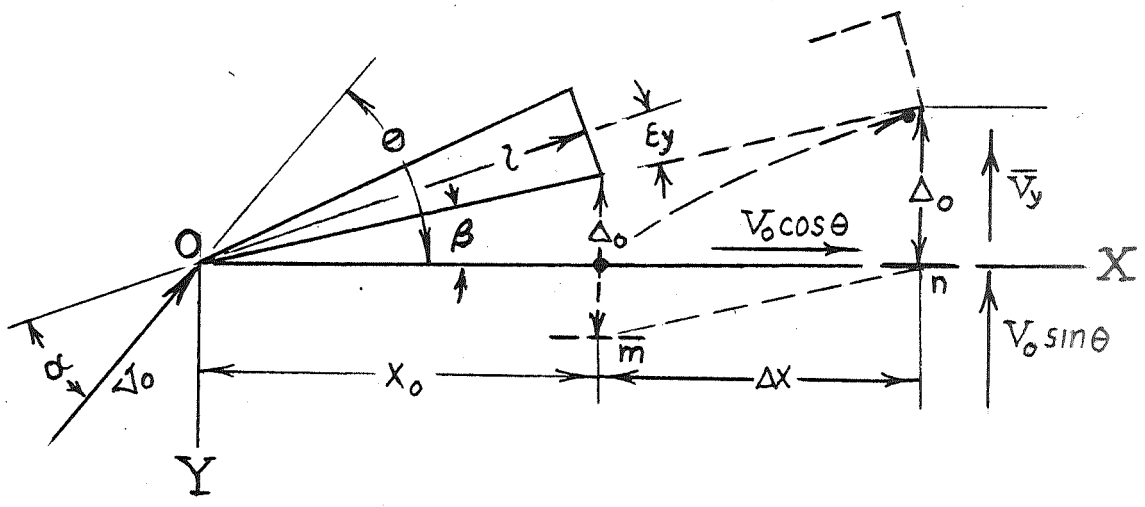

Sketch (a)

Sketch (a) depicts a conical body with its upper surface element in the vertical plane of symmetry defining an angle, β, with respect to the shock trace, OX, which is inclined at the angle, θ, with respect to the free stream-direction. If the horizontal component of velocity, $V_o\cos\theta$, were neglected, the shock stand-off distance, Δ_o, from the base of the body at location x_o to a "virtual" shock location, element m, is established by two-dimensional shock applied to the local body cross-section in the normal flow field. When the horizontal component of velocity is considered, the stand-off distance, Δ_o, is maintained with respect to an extension of the body surface element but is translated a distance, Δx, so that the virtual shock element, m, appears at the real location, n, on the shock trace, OX, this position being occupied with respect to a transformed (elongated) body. Since the value, Δ_o, is established, the angle, β, may be determined using the length of the transformed body, $x_o + \Delta x$, as follows:

The Y-components of the stream velocity in the shock layer varies from the value immediately behind the shock, $\frac{\rho_o}{\rho_\theta} V_o\sin\theta$, to the value approaching the body surface, $V_o\cos\theta\tan\beta$. The average velocity $\overline{V}_y = \frac{1}{2}V_o(\frac{\rho_o}{\rho_\theta}\sin\theta + \cos\theta\tan\beta)$. The X-component of velocity is $V_o\cos\theta$. Therefore, a stream particle commencing from the shock at location x_o is carried the horizontal distance, Δx, with velocity, $V_o\cos\theta$, in the time interval required for it to approach the transformed body at Y-distance, Δ_o, with the average velocity, $\overline{V}_y$. Thus-

$$\frac{\Delta_o}{\Delta x} = \frac{\overline{V}_y}{V_o\cos\theta} = \frac{1}{2}(\frac{\rho_o}{\rho_\theta}\tan\theta + \tan\beta) \quad \ldots\ldots\ldots\ldots\ldots\ldots\ldots \quad (6)$$

By inspection of sketch (a)

$$\Delta_o - x_o\tan\beta = \Delta x\tan\beta \quad \ldots\ldots\ldots\ldots\ldots\ldots\ldots\ldots\ldots \quad (7)$$

Substitutuon of equation (7) into equation (6) give -

$$\tan\beta\left(\tan\beta + \frac{\rho_o}{\rho_\theta}\tan\theta\right) + \frac{\Delta_o}{x_o}\left(\tan\beta - \frac{\rho_o}{\rho_\theta}\tan\theta\right) = 0 \quad \ldots\ldots\ldots (8)$$

x_o is related to the cone geometry as follows:

$$\frac{l}{\cos\varepsilon_y} = \frac{x_o}{\cos\beta}\ , \quad b = l\tan\varepsilon_z,\ a = l\tan\varepsilon_y$$

$$\frac{1}{x_o} = \frac{\tan\varepsilon_z \cos\varepsilon_y \sec\beta}{b} \quad \ldots\ldots\ldots\ldots\ldots (9)$$

Substitution of the above value for X_o into equation (8) gives the final result -

$$\tan\beta\left(\tan\beta + \frac{\rho_o}{\rho_\theta}\tan\theta\right) + \frac{\Delta_o \tan\varepsilon_z \cos\varepsilon_y \sec\beta}{b}\left(\tan\beta - \frac{\rho_o}{\rho_\theta}\tan\theta\right) = 0 \quad \ldots\ldots (10)$$

Equation (10) give β as a function of θ, however, the angle, β, as a function of angle of attack, α, is readily found through the relationship - $\alpha = \theta - \beta - \varepsilon_y$ (sketch (a)).

For small values of β ($\sec\beta = 1$), equation (10) can be formed as a quadratic equation and an approximate solution readily obtained. The exact solution in chart form is presented in figure 1, wherein β is plotted as a function of $(\Delta_o/b)\tan\varepsilon_z\cos\varepsilon_y$ for various parameter values $\frac{\rho_o}{\rho_\theta}\tan\theta$. The required value, Δ_o/b, is the shock solution for two-dimensional cylinders and is a function of the shock density ratio and the body cross-section. Solutions for various elliptic cross sections and slab sections with round corners are given in figure 2. These solutions are from an unpublished method which is a two-dimensional extension to the axisymmetric solutions of reference 7. The discontinuities in the solutions are due to arbitrary step changes in the value of the gas specific-heat ratio, γ,

at $\rho_\theta/\rho_o = 6$ and 11. The effect of γ may be estimated by interpolation if some "real gas" γ can be specified.

EXAMPLE APPLICATION

The following numerical example illustrates the calculative procedure and use of the charts herein included to determine the shock angle and pressure coefficient solutions for a typical conical body at an angle of attack in air ($\gamma = 1.4$) at Mach number 5.

Given $a/b = 1/3$, $\varepsilon_z = 15^o$, ($\varepsilon_y = 5.10^o$), and $M_o = 5$; determine the angle of attack and pressure coefficient when the shock is inclined ($\theta = 60^o$) to the free stream. The shock density ratio, $\frac{\rho_o}{\rho_\theta}$, across the oblique shock with $\gamma = 1.4$ is first determined -

$$\frac{\rho_o}{\rho_\theta} = \frac{(\gamma-1)}{(\gamma+1)} + \frac{2}{(\gamma+1)M_o^2 \sin^2\theta} = \frac{.4}{2.4} + \frac{2}{2.4x25x.750} = .211$$

The reciprocal value, $\frac{\rho_\theta}{\rho_o} = 4.74$. Figure 2(a) gives the value $\Delta_o/b = .692$ at $\frac{\rho_\theta}{\rho_o} = 4.74$ for an elliptic section with $a/b = 1/3$.

Quantities required in figure 1 are now evaluated. The abscissa value $(\Delta_o/b)\ \tan\varepsilon_z \cos\varepsilon_y = .692x.268x.996 = .185$. The parameter, $\frac{\rho_o}{\rho_\theta}\tan\theta = .211x1.732 = .366$. The above values intersect on the curves of figure 2(a) at the ordinate value, $= 5.85^o$. The angle of attack, $\alpha = \theta - \beta - \varepsilon_y = 60^o - 5.85^o - 5.10^o = 49.05^o$

The pressure coefficient, equation (5) is evaluated -

$$C_p = \frac{4.4}{2.4} \times .750 - \frac{2}{2.4 \times 25} - .500 \times .866 \times .1025 = 1.297$$

Note that a specific angle-of-attack value cannot be selected a priori. Calculations with several values of θ can be made quickly, however, and curves of C_p and β constructed as functions of angle of attack. The above procedure also applies to round corner slab sections where r_c takes the role of "a" (figure 2(b)).

EXTENSION OF THE METHOD

A delta wing-body configuration is depicted by solid outline in figure 3. The dashed lines represent outlines of a series of tandem cone frustums with which the configuration shape is approximated. The cone elements are constructed tangent to the bottom surface at the vertical plane of symmetry and are also made tangent to the planform outline of the configuration as indicated. A typical cross section meeting these requirements is shown. Cross sections varying from a circle to ellipses of increasing ellipticity and several round-corner slab sections were utilized in the construction of figure 3. Thus, the actual configuration is approximated by a series of cone frustums of step-wise varying cross section, apex angle, and angle of attack. The accuracy of the approximation increases with the number of frustums used.

Calculations of pressures and shock angles are then made for the individual cones in the manner of the above example calculation. The shock layer thickness is then determined by integration of the local shock angles (appropriate to each cone) plotted as a function of body surface length.

$$\Delta_s = \int_o^s \beta ds = \int_o^s \left(\frac{d\Delta}{ds}\right) ds \quad \ldots\ldots\ldots\ldots\ldots\ldots \quad (11)$$

Equation (11) may be integrated either by graphical or tabular methods.

COMPARISON BETWEEN EXPERIMENTAL AND THEORETICAL RESULTS

A comparison between experimental and predicted centerline shock layer thickness for a delta wing-body configuration at $M_o = 7.4$ is included in figure 3. Experimental and predicted values are in good agreement.

Note that the shock layer thickness has the same value at the angles of attack 15^o and 30^o. Comparisons of experimental and predicted results for elliptic cones are presented in figure 4. A wide range in cone geometry and Mach number ($3 < M_o < 10$) is represented. The useful angle of attack range of the method is restricted in that when the centerline shock trace incline approaches $\theta = 90^o$ the angle β approaches the approximate value $\frac{\Delta_o}{b}\epsilon_z$. The limiting angle of attack is then $\alpha \approx 90^o - \frac{\Delta_o}{b}\epsilon_z - \epsilon_y$. Thus, α reaches the highest value for slender cones (small ϵ_z and ϵ_y) and, for cones of a given slenderness, has higher values with increasing Mach number (decreasing Δ_o/b). Agreement between experimental and predicted values is generally within 10% and is particularly satisfactory at the higher Mach numbers. The data at Mach numbers, 2.94, 3.87, and 4.78 are previously unpublished results of tests in the Ames 1- by 3-foot wind tunnel.

Figure 5 presents a comparison between experimental and predicted centerline pressure distributions for the delta wing-body configuration shown in figure 3. Agreement is satisfactory at angles of attack up to 30^o. At the angle of attack of 40^o a discrepancy between experimental and predicted pressures occurs over a portion of the body length, however, the predicted values given by the present method are in better accord with experiment than are the indicated results of modified Newtonian theory.

A comparison between experimental and predicted centerline pressures for cones is presented in figure 6 in the form of a correlation curve. The range of angle of attack, Mach number, and configuration cross sections are noted on the figure. Experimental and predicted values correlate within the limits of about ± 2 percent.

CONCLUDING REMARKS

Simple methods were developed for prediction of inclination of a shock with respect to the windward trace on a conical surface in the vertical plane of symmetry and for estimation of pressure coefficient on this body trace.

Predicted values were compared with experiment for air flows in the Mach number range 3 to 10 and the angle of attack range of 0° to about 70° for cones of a wide range in geometry. The methods were extended to the prediction of vertical symmetry plane shock layer thicknesses and body surface pressures of configurations with arbitrarily changing cross-sections with body length by the use of a tandem series of locally conical elements to approximate the body shape. This, in effect, is a refined tangent cone procedure.

The applicability of the methods have been demonstrated by comparison with test results from low enthalpy air flows. The suitability of the method for real gas flows is believed valid also since the real gas effect enters primarily through the density ratio across the shock.

REFERENCES

1. Van Dyke, Milton D., and Gordon, Helen D.: Supersonic Flow Past a Family of Blunt Axisymmetric Bodies. NASA Technical Report R-1, 1959.

2. Fuller, Franklyn B.: Numerical Solutions for Supersonic Flow of an Ideal Gas Around Blunt Two-Dimensional Bodies. NASA TN D-791, 1961.

3. Rakich, John V.: A Method of Characteristics for Steady Three-Dimensional Supersonic Flow with Application to Inclined Bodies of Revolution. NASA TN D-5341, 1969.

4. Bazzhin, A. P.: The Calculation of Supersonic Flow Past a Flat Plate with a Detached Shock Wave (Unpublished work performed at the Computing Center Academy of Sciences, U.S.S.R.). Translated by Ronald F. Probstein, Massachusetts Institute of Technology, 1963.

5. Cleary, Joseph W.: Approximation for Distribution of Flow Properties in the Angle of Attack Plane of Conical Flows. NASA TN D-5951, 1970.

6. Kaattari, George E.: A Method for Predicting Pressures on Elliptic Cones at Supersonic Speeds. NASA TN D-5952, 1970.

7. Kaattari, George E.: A Method for Predicitng Shock Shapes and Pressure Distributions ofr a Wide Variety of Blunt Bodies at Zero Angle of Attack. NASA TN D-4539, 1968.

8. Palko, R. L., and Ray, A. D.: Pressure Distribution and Flow Visualization Tests of a 1.5 Elliptic Cone. Report No. AEDC-TDR-63-163, 1963.

9. Randall, R. E., Bell, D. R., and Burk, J. L.: Pressure Distribution Tests of Several Sharp Leading Edge Wings, Bodies, and Body-Wing Combinations at Mach 5 and 8. AEDC-TN-60-173, 1960.

10. Bernot, Peter T.: Pressure Distributions on Blunt Delta Wings at Angle of Attack up to 90°. NASA TN-D-1954, 1963.

11. Squire, L. C.: Pressure Distributions and Flow Patterns at M=4.0 on Some Delta Wings. Ministry of Aviation, Aeronautical Research Council Reports and Memoranda, 1964.

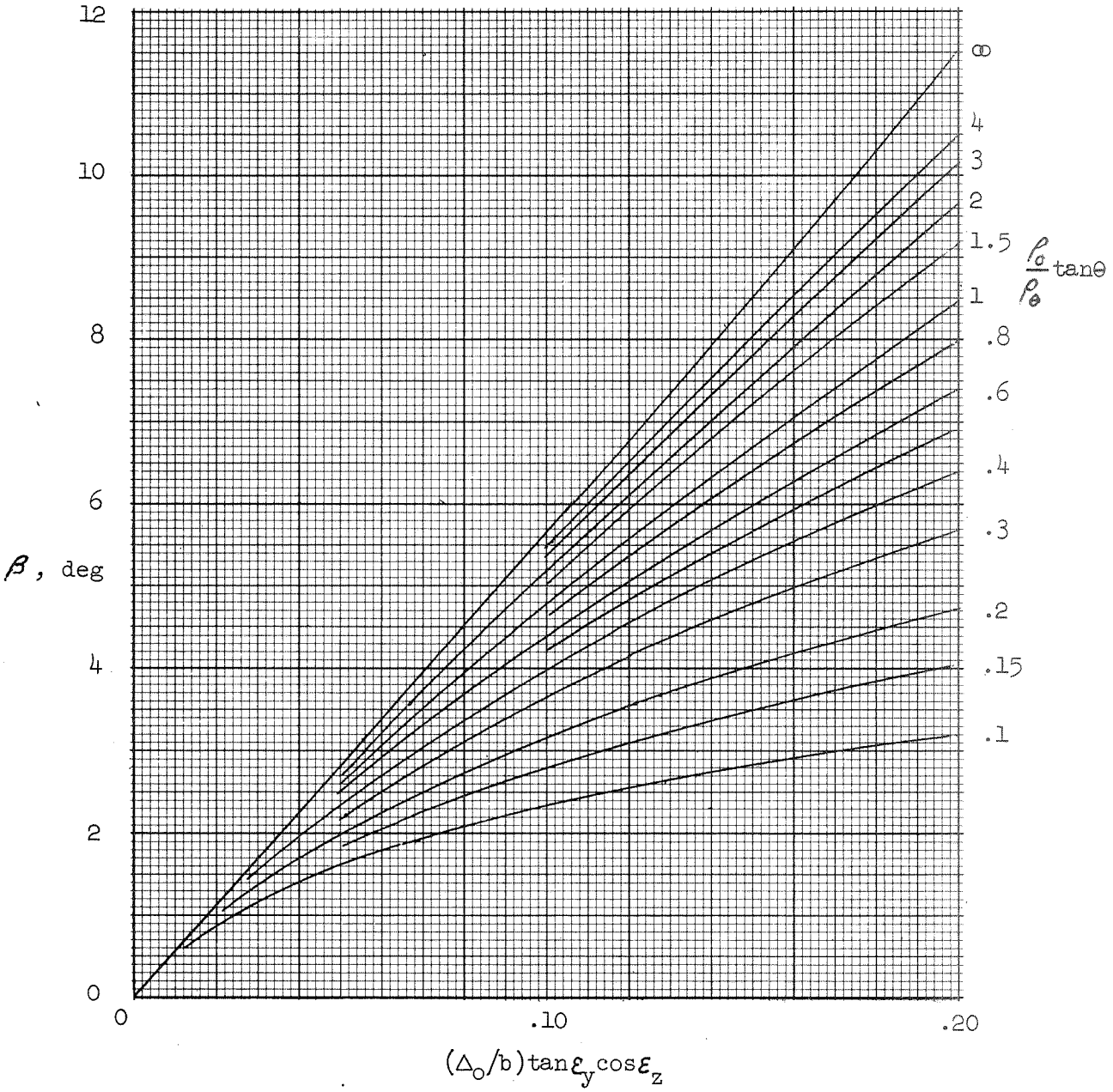

(a) $(\Delta_o/b)\tan\varepsilon_y\cos\varepsilon_z = 0$ to 0.20

Figure 1.- Solutions of equation (10) for the angle β.

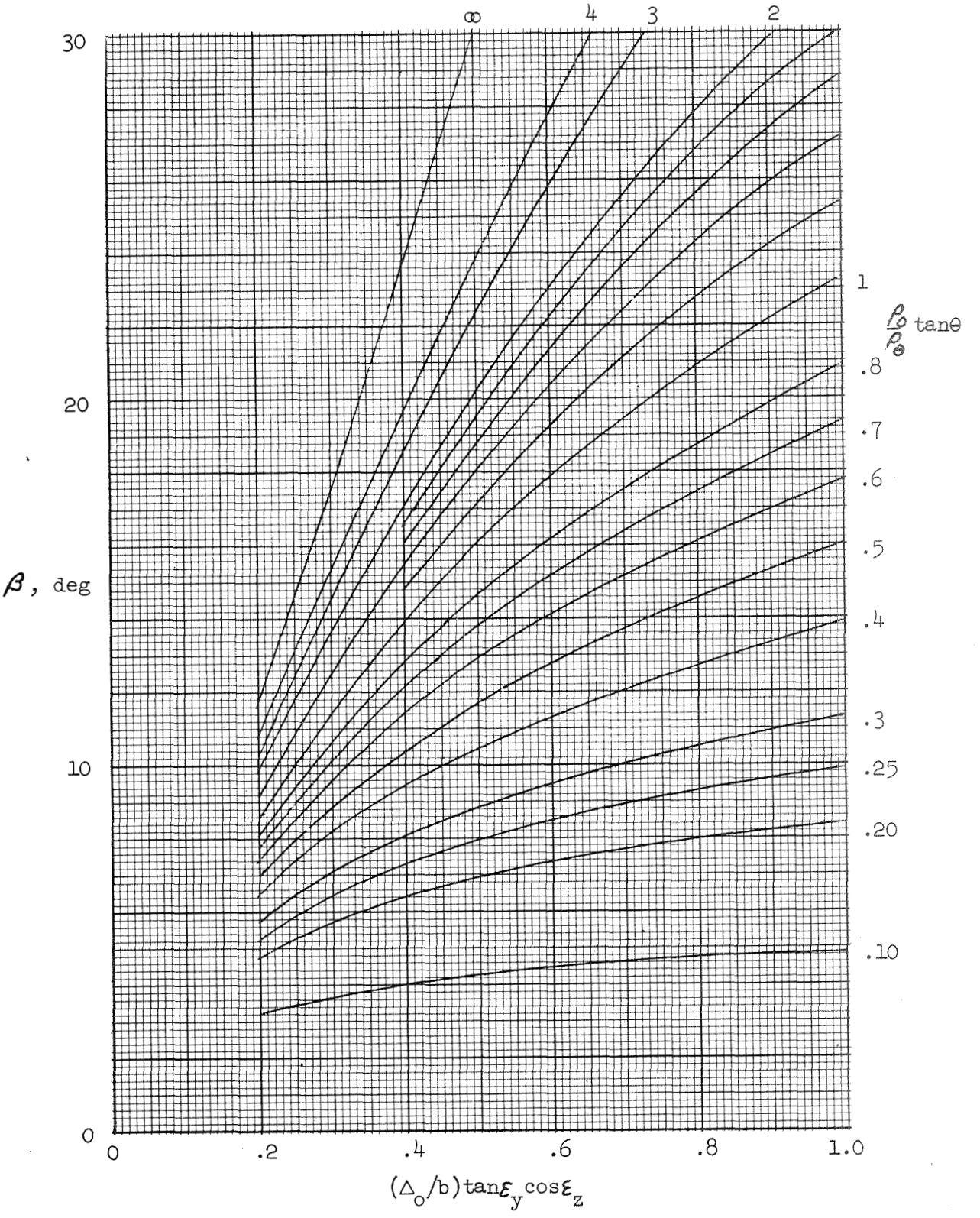

(b) $(\Delta_o/b)\tan\varepsilon_y\cos\varepsilon_z$ = .2 to 1.0

Figure 1.- Concluded

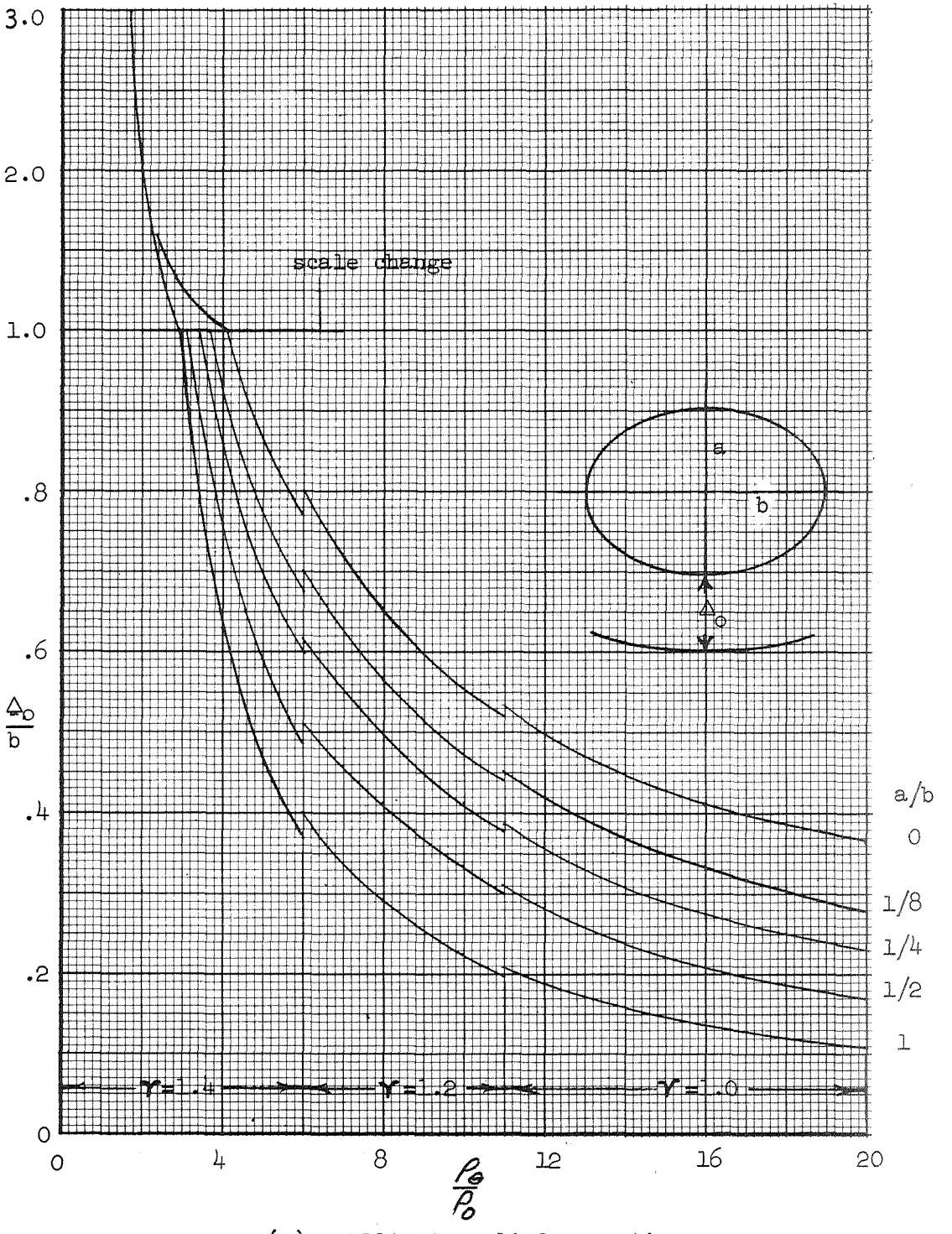

(a). Elliptic cylinder sections

Figure 2.- Centerline shock standoff

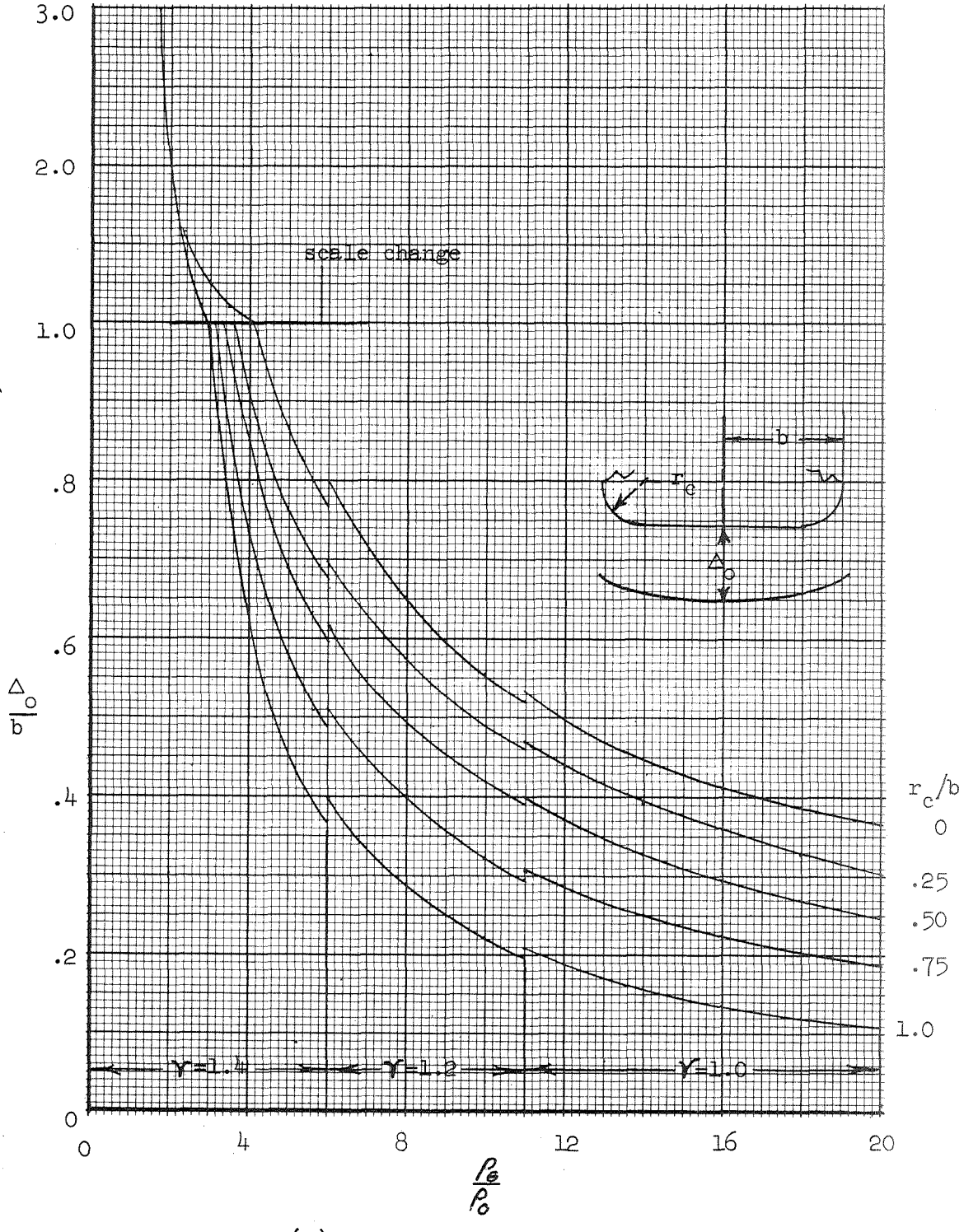

(b). Round-corner slab sections

Figure 2.- Concluded.

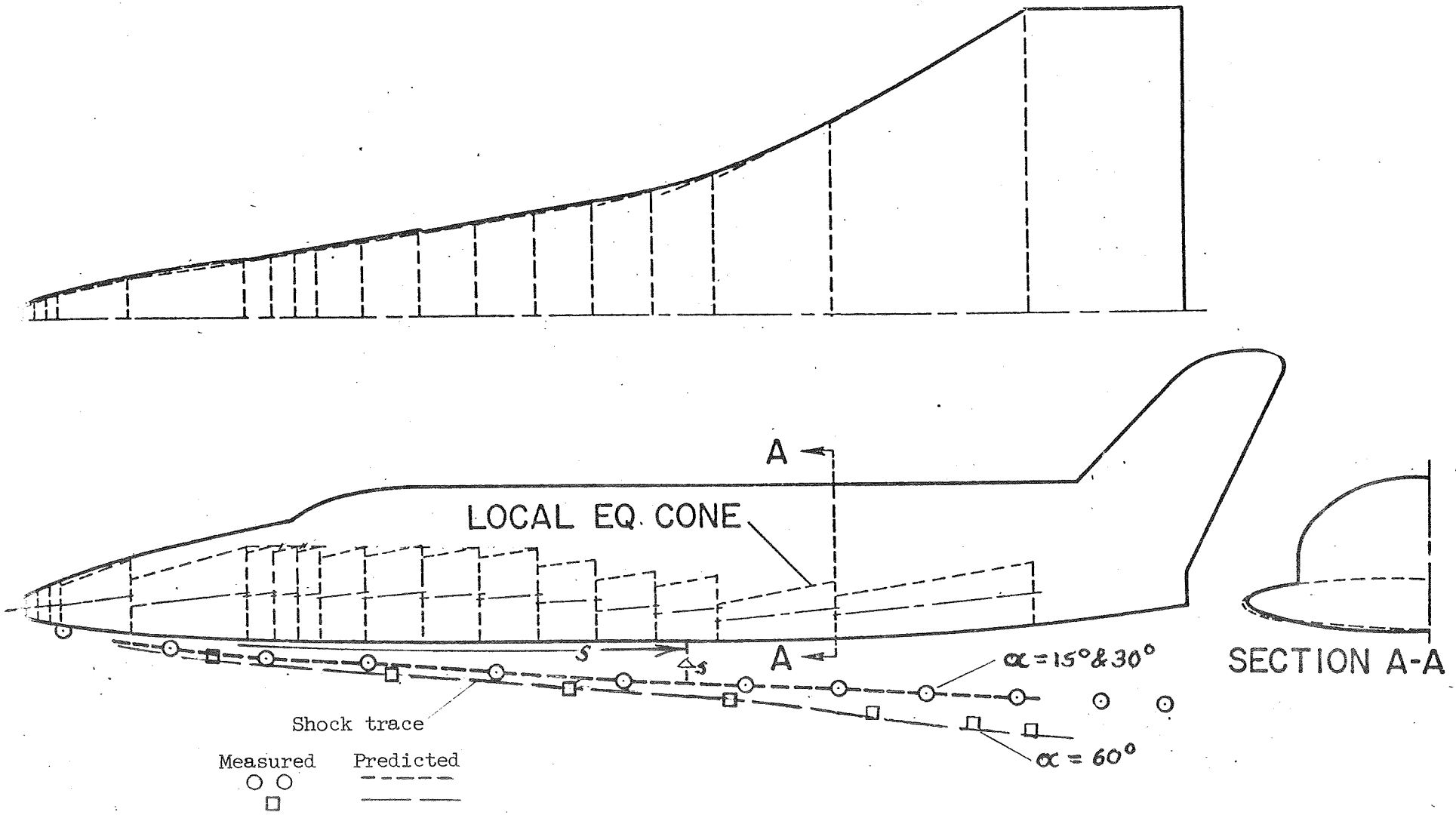

Figure 3.- Approximation of delta wing-body by cone frustums and comparison of measured and predicted shock shapes, $M_o = 7.4$.

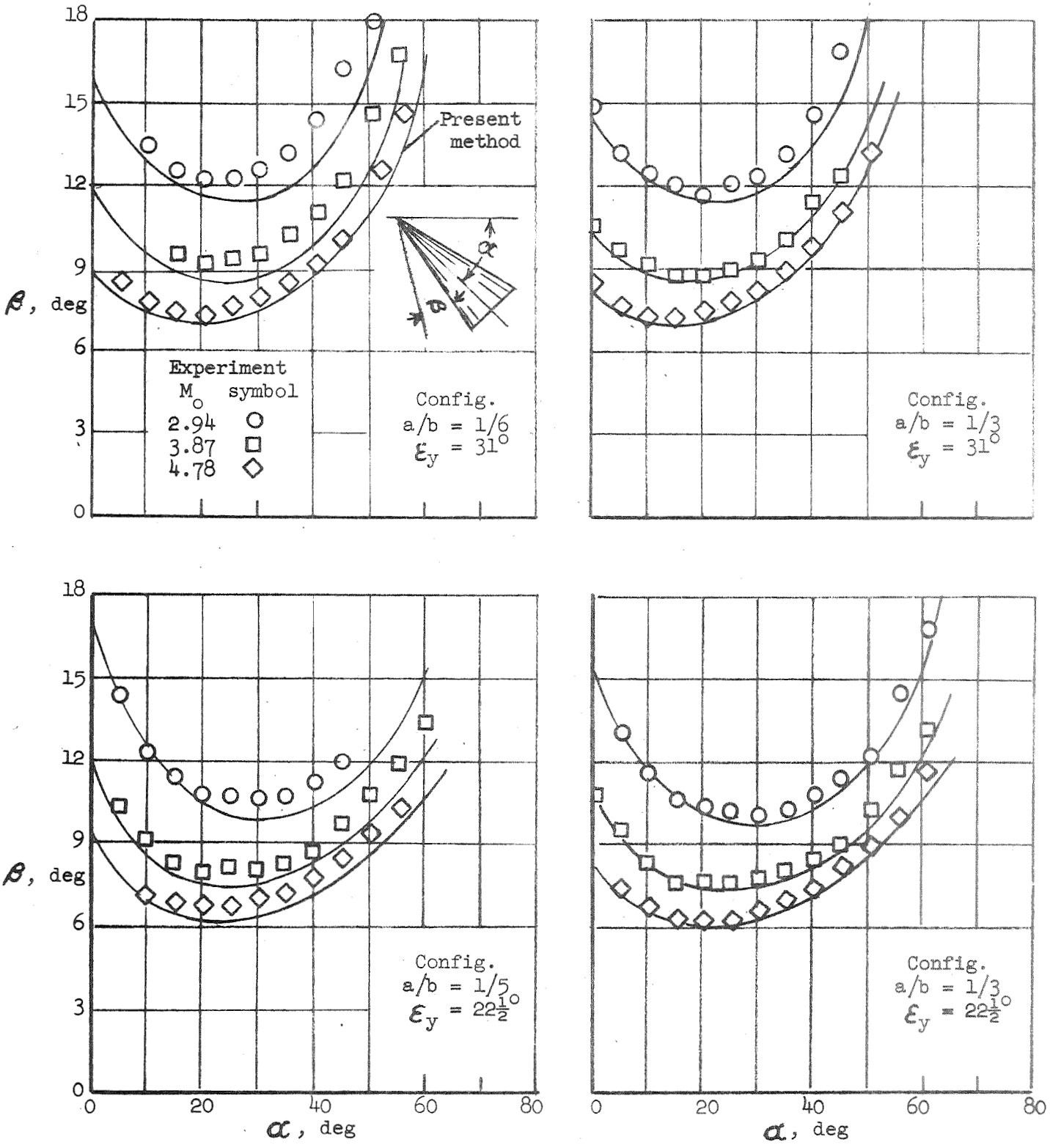

Figure 4.- Experimental and predicted values of β as a function of angle of attack, α.

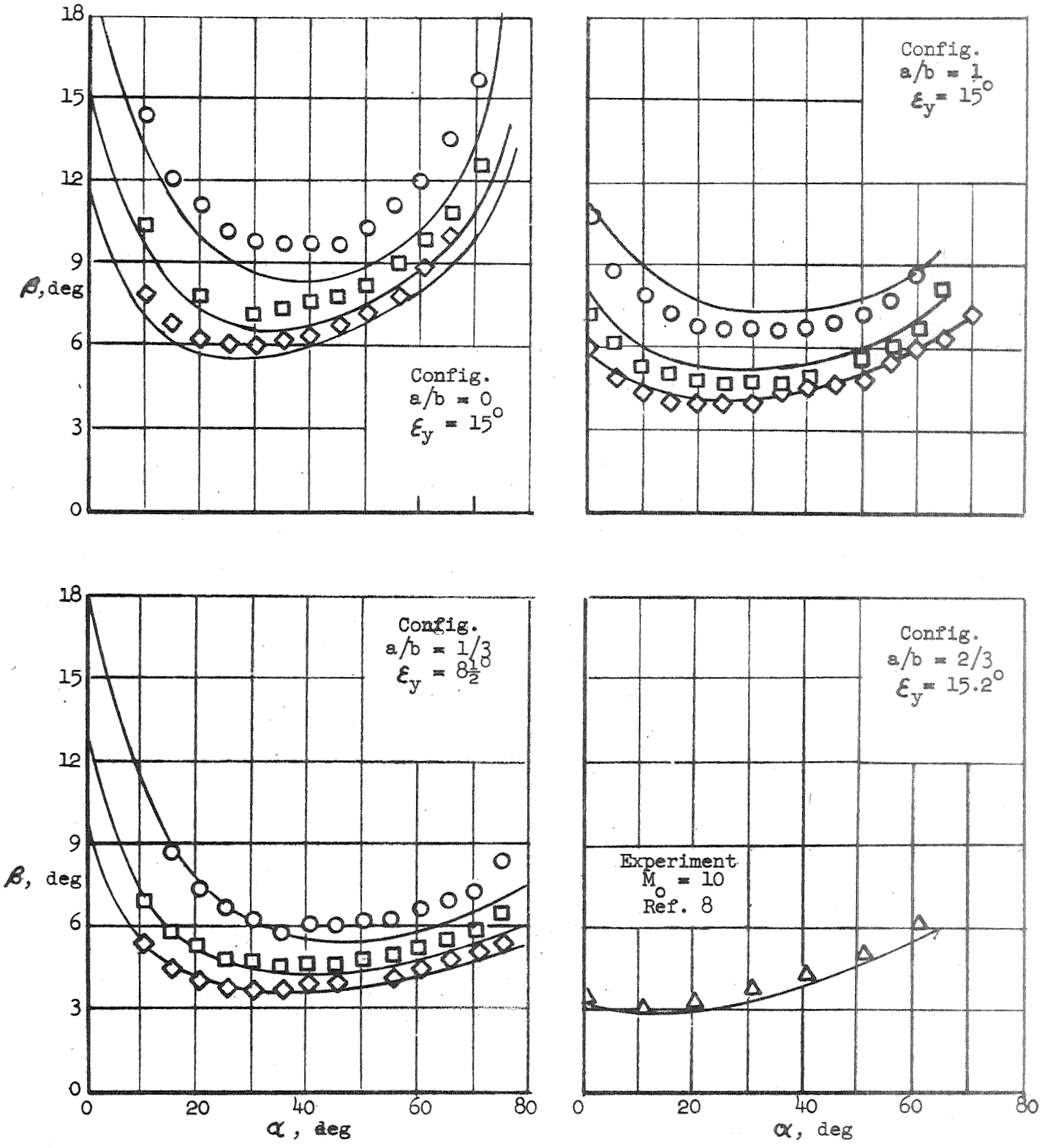

Figure 4.- Concluded.

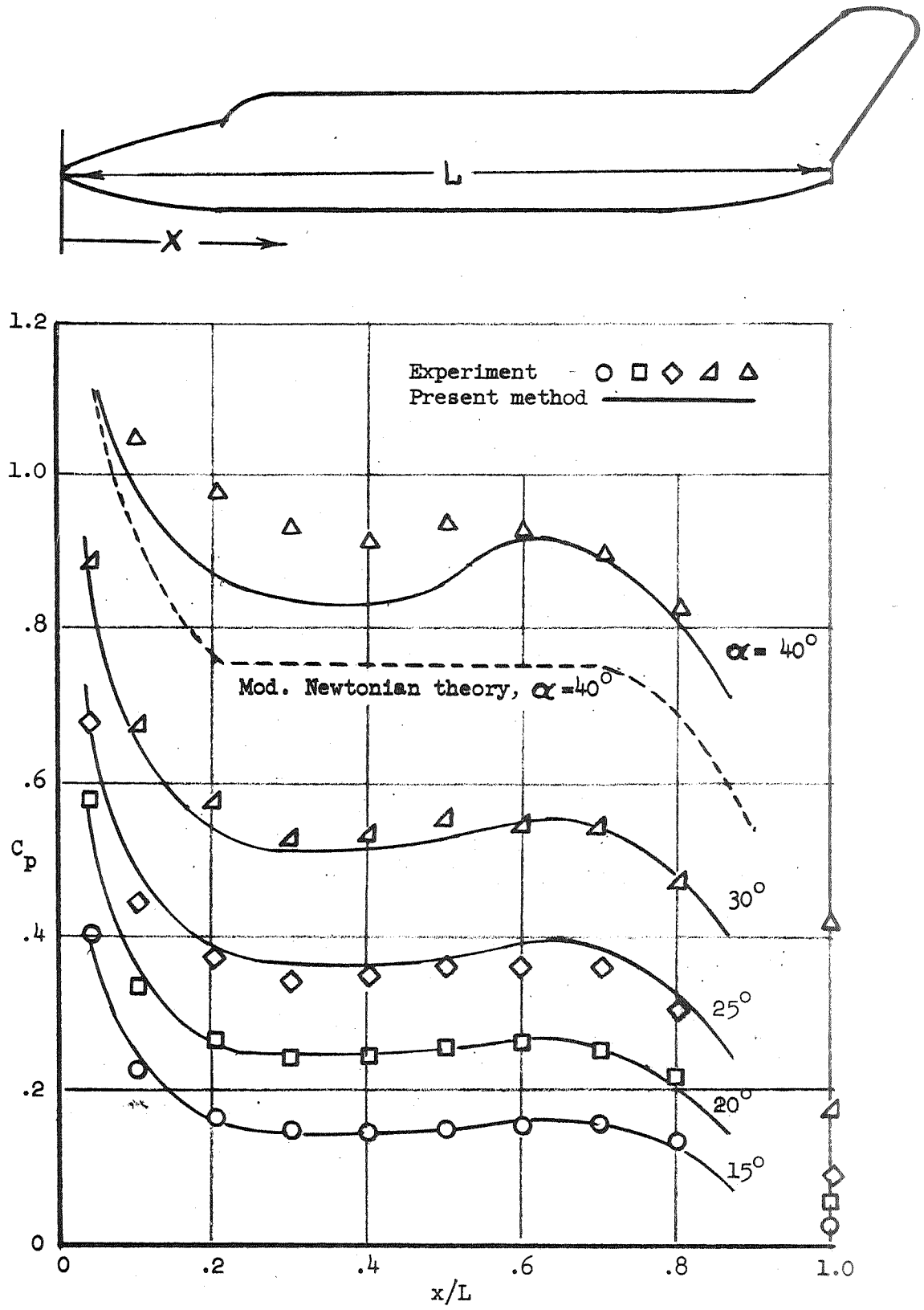

Figure 5.- Experimental and predicted pressure distributions on delta wing-body configuration, M_o = 7.4.

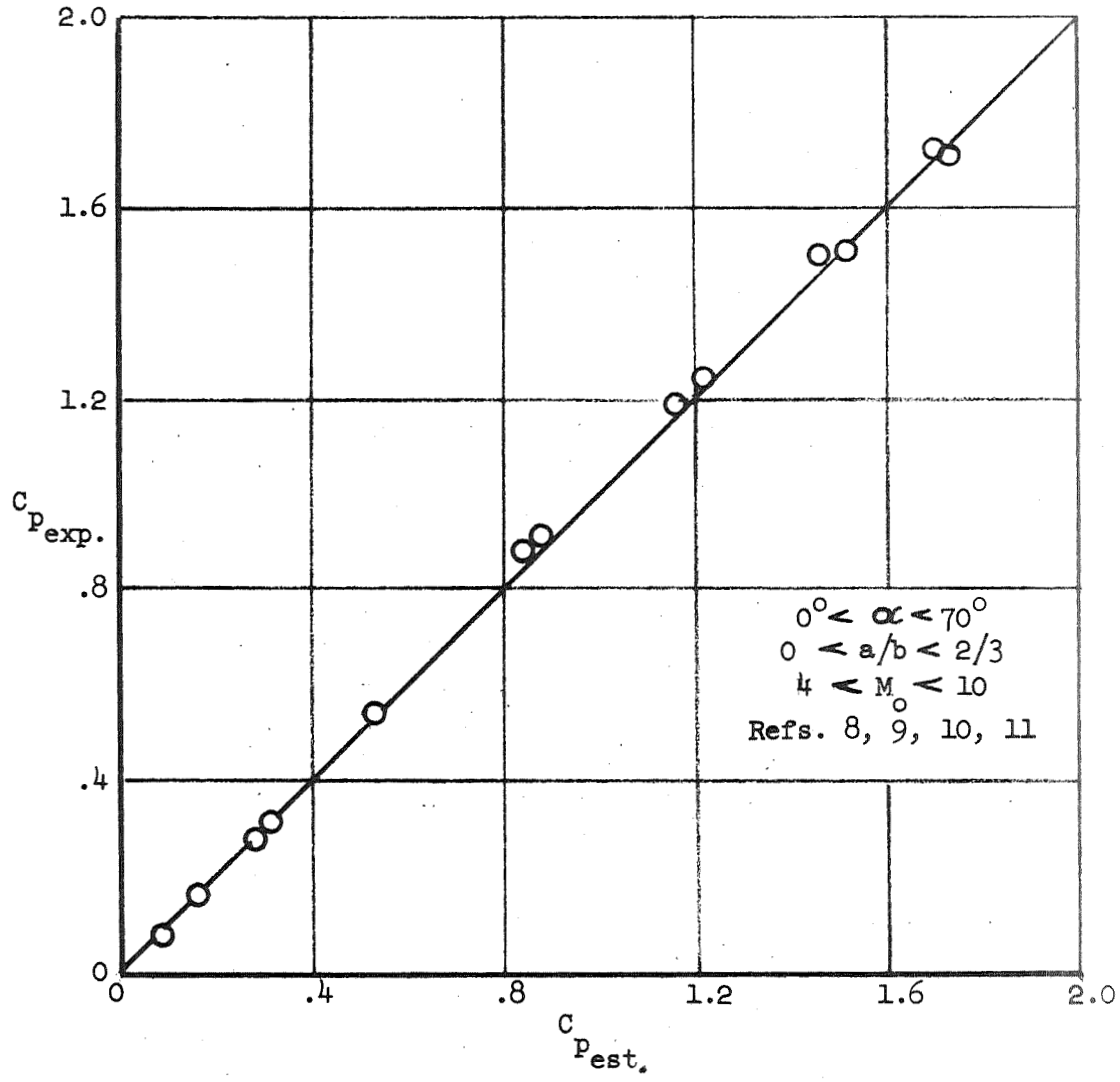

Figure 6.- Correlation of experimental and predicted centerline pressure coefficients on cones.